CRATER FORMATION DURING THE ONSET OF MUD VOLCANISM

*[1]Evan Pryce, [1]Chris Kirkham and [1]Joe Cartwright

[1]Department of Earth Sciences, University of Oxford, South Parks Road, Oxford, OX1 3AN, UK

*Corresponding author
Email: evan.pryce@st-annes.ox.ac.uk

Abstract

Three-dimensional (3D) seismic imaging is used to reveal >2.5km wide and >150m deep craters at the basal surface of 64 mud volcanoes out of a suite of 86, offshore Egypt. The craters were infilled soon after they formed by successive mud extrusions that combined to build mud volcanoes, as evidenced by onlap fill geometries of the earliest mud flows. We propose that the craters formed as the earliest manifestation of mud volcano formation. We infer that the energy required to excise in situ clays and sands buried and consolidated to depths of over 150m below the seafloor was provided by the highly vigorous venting of a dominantly gas and water mix during the initial eruption, in which gas column height was the critical factor. This primary phase of mud volcanism is rarely observed and the findings presented here have significant implications for how we view the dynamism of this fundamental stage of mud volcano genesis.

Introduction

Mud volcanoes are found in convergent and passive marine and terrestrial sedimentary basins globally, and are formed by remobilisation and venting of overpressured regions (Mazzini and Etiope, 2017; Milkov, 2005). The eruptive flux can be highly gas-rich, sometimes resulting in extrusive episodes where the gas ignites explosively close to the surface producing gas flares (Mazzini et al., 2021). Mud volcanoes have wide significance for society (Tingay et al., 2015) both as geohazards in their own right (e.g. the Lusi eruption, whose mud flow displaced >30,000 people (Davies et al., 2008; Mazzini et al., 2007)), and as natural valves for significant methane emission to the atmosphere (>15Mt/yr.; Mazzini and Etiope, 2017).

One of the most poorly documented aspects of mud volcanism is the nature of the initial eruption that presages the construction of the mud volcano. The initial eruptive phase is critical for understanding the triggering mechanism for the fluid-sediment remobilisation. This initial eruptive phase has only rarely been documented, either from eye-witness accounts of newly-forming mud volcanoes (Barr and Bolli, 1953; Higgins and Saunders, 1974) or from analysis of cores of the first extrusive flows at the bases of drilled mud volcanoes (Kopf et al., 1998; Robertson, 1996).

In this study, we use high-resolution 3D seismic reflection imaging of a suite of 86 recently erupted mud volcanoes (MV) in one of the most MV-dense regions on Earth, the El Dabaa Mud Volcano Province, offshore Egypt (Kirkham et al., 2017). Our data images both the basal surface and the internal stratification of these recently erupted MVs, allowing analysis of their extrusion geometry and basal configuration to provide new insights into the initial conditions for mud volcanism.

Geological setting

The study area is in the western Nile Deep Sea Fan at water depths of 2500-3000m (Fig. 1A). A >1km thick and regionally extensive layer consisting predominantly of halite (Messinian Evaporites; Figs. 1A & 1B) was rapidly deposited in the basin during the Messinian Salinity Crisis (Krijgsman et al., 1999; Ryan, 2009). The salt primed the development of high overpressures in the underlying clastic Oligo-Miocene succession (Fig. 1B) (Dolson, 2020). The overpressured Miocene interval comprises mainly claystones with some thin turbiditic sands in slope channels or overbank deposits (Dolson, 2020; Kellner et al., 2018). The Pliocene-Recent post-salt comprises deepwater fine grained hemipelagic deposits and coarser grained turbidite deposits locally (Loncke et al., 2004).

Data and methods

The 3D seismic reflection data used in this study include pre-stack time and depth migrated surveys that cover the same c.4300km^2 area (see the Supplemental Material for further details on the seismic data). The key horizons of the Seafloor, Top Salt and Base Salt, as well as the top, base and internal reflection geometry of 86 MVs were picked manually and autocorrelated over local areas to allow dimensions and stratigraphic features to be recorded (Figs. 1C & 1D; Table S1). Measurements of the diameter and relief of surfaces interpreted at the bases of the MVs were recorded using the Petrel measuring tool (Table S1). Error in measurements are a function of the seismic lateral resolution (c.25m) and vertical resolution (c.10m).

The El Dabaa Mud Volcano Province

The El Dabaa Mud Volcano Province contains >400 MVs erupted in the past 5Ma and distributed throughout the Pliocene-Recent succession over an area of >4000km^2 (Fig.

1D; Fig. S1) (Kirkham et al., 2017; Mascle et al., 2014). The MVs range from 550-5650m in diameter, with a generally circular planform. They are identified in the seismic data from their distinctive high amplitude upper and basal surfaces that consistently converge to a single merged seismic reflection at their lateral margins that can be used to relatively date the age of the MV (Figs. 1D, 2A & 2B; Figs. S1-3). The time taken to form each MV can only be estimated as taking less than ~200kyrs based on the time represented by these merged reflections at the lateral margins and assuming an average sedimentation rate throughout the past 5Ma (Fig. 1D) (Kirkham et al., 2017). The MVs are best preserved and imaged when erupted at or near the present seafloor (Fig. 1D). Older MVs display more irregular geometries due to compaction, deformation by salt tectonics and localised subsidence above the site of mud withdrawal in the pre-salt (depletion zone) associated with younger adjacent MVs (Fig. 1D) (Kirkham et al., 2017). Gross volumes range from $4\text{x}10^6$-$3.3\text{x}10^9\text{m}^3$.

The upper surface of the MVs typically builds modest relief of tens of metres at the seafloor, or more rarely hundreds of metres, with flank dips of <5°, and either a conical summit or a summit crater (Figs. 1D, 2A & 2B). The majority of their basal surfaces have a pronounced concave downward geometry and a subset of these are also characterised by crater-like features (Figs. 1D, 2A & 2B; Fig. S3).

Pipe-like conduits have been identified for many of the MVs in El Dabaa (Fig. 2B) and link the depletion zone with the extruded MV (Kirkham et al., 2018). These conduits initially emanate from the crest of stratigraphic traps at the Base Salt that contain parallel stratified layers, are sealed above and laterally by the salt and are later modified by mud depletion (Fig. S4) (Kirkham et al., 2022).

The basal surfaces of the mud volcanoes

Of the ~400 MVs identified in El Dabaa we focus here on a subset of 86 that are located at the seafloor and hence undeformed (Fig. 1C). The basal surfaces were classified into two types (Fig. 1C; Table S1): those with craters that truncate the underlying substrate (Figs. 2A & 2C; Fig. S2A) and those without (Figs. 2B & 2D; Fig. S2B). A clear majority of MVs were found to have craters, comprising 74% of the total. We observed the following general characteristics in the basal surfaces with craters (Figs. 2A & 2C): (1) a broad bowl shape in 3D, circular to irregular planform that is centred on the underlying conduit; (2) concentric truncation of underlying Pliocene-Recent reflections by the crater; (3) crater extent much greater than the diameter of the conduit but less than the MV diameter; (4) local scarp irregularities along the crater margins. Where internal reflections of the MVs are visible (Fig. 2A; Fig. S3), these can be seen to infill the basal craters with an onlap or downlap geometry. Crater relief ranges from 15-160m with diameters of 200-2850m and exhibits a positive correlation ($R^2 = 0.52$) suggesting a modest scaling between these parameters (Fig. 2E; Table S1). The bulk volume of near seafloor sediments removed from the craters ranges from 1.6×10^5-$2.8 \times 10^8 m^3$. There is no evidence of deposits beyond the crater rims that could represent remnants of this excised material. The basal craters are not underlain or offset by any faults (Figs. 2A & 2B).

The basal surface of MVs without craters contrast with those that do in that they do not truncate the underlying substrate and are parallel to the underlying stratal reflections. Their edifices have comparable geometries and parameters (Figs. 2B & 2D).

Discussion

The key observations may be summarised as relating to the geometrical relationships between the basal surfaces of the MVs with craters, their truncated substrates and fill stratigraphies. What process could explain our observations? We consider five possibilities:

(1) MV growth rate equal to background sedimentation rate; (2) shallow mud chamber inflation, seafloor folding and erosion; (3) local caldera collapse; (4) vigorous initial eruption; and (5) slumping and failure. We argue against the first three for the following reasons:

(1) Crater diameter is always significantly less than mud edifice diameter and there is no evidence of interdigitation between the mud edifice and background stratigraphy (Fig. 2A; Fig. S3).

(2) From the suite of >400 MVs in El Dabaa, no shallow mud chambers have been observed feeding the surface extrusions (Kirkham et al., 2017).

(3) The absence of ring faults precludes a genesis associated with caldera-style collapse (Figs. 2A & 2C) (Stewart and Davies, 2006).

Crater formation by a highly vigorous initial eruption (4) would involve the geologically instantaneous removal of the truncated material by venting at the seafloor, thereby generating negative relief prior to edifice construction (Fig. 2A; Fig. S3). The consistent interpretation of basal craters vertically aligned with mud cones at the upper surface of MVs and conduits (apart from when obscured by image resolution) (Kirkham et al., 2018) indicates that crater genesis is directly related to the processes of mud volcanism, particularly venting from the conduit during the initial onset of mud volcanism (Fig. 3). Excavation by a highly vigorous eruptive process would explain the stratigraphic and spatial relationships and be capable of incising up to 150m downward into stiff clays of the substrate (Figs. 2A & 2C; Fig. S3). This process must disperse the erosional products far-afield, otherwise accumulations of the exercised material should be observed around the crater flanks (Fig. 2A). In the context of geometric evolution, the formation of craters during phreatomagmatic eruptions (Geshi et al., 2011) or of pockmark craters (Fig. S4) (Løseth et al., 2011) present suitable analogues. Examples of pockmark craters with some mud fill in El Dabaa (Fig. S4) show a striking resemblance to the basal craters (Fig. 2A; Fig. S3).

Slumping and slope failure (5) alone cannot explain the crater formation, because a process to remove material and reduce confining stress is first required. However, formation of the craters at the seafloor, their occasionally irregular planform, arcuate scarps and modest R^2 value between crater diameter and relief (Figs. 2A, 2C & 2E) collectively could point to some retrogressive local slope failure from an initial locus that modifies the crater to its final geometry (Fig. 3B). The initial phase of mud extrusion and edifice construction follows, with no intervening drape of any locally reworked surficial sediments (Figs. 2A & 3C). Any failed slope material must therefore have also been ejected from the crater.

Previous works have inferred from core studies of basal units in MVs that their initial phase of genesis is a vigorous eruption of mainly fluids, principally water and methane (Deville and Guerlais, 2009; Kopf et al., 1998; Robertson, 1996). Eye-witness accounts of newly erupting MVs in Trinidad report that the formation of several mud volcanic islands in the 20th century was preceded by vigorous, and voluminous eruptions of water and methane (Barr and Bolli, 1953; Higgins and Saunders, 1974). In the Erin Bay eruption, 1911, the initial violent eruption of fluids and gas lasted only a few hours, and was followed by mud slurry and muddy breccia extrusions that built the island edifice (Kugler, 1933). The overpressuring effect of a geologically instantaneous eruptive flux that is dominated by water and free gas could provide the energy for a vigorous initial eruptive phase capable of remobilising and eroding near surface sediments to form a crater (Figs. 3A & 3B).

Why should the initial flux be dominantly composed of methane and water? There is an abundance of shallow gas anomalies within and adjacent to the MVs in El Dabaa (Fig. S5) and thermogenic and biogenic gas sourced from the pre-salt has been directly sampled from their extrusive brines (Loncke et al., 2004; Prinzhofer and Deville, 2013). The source region for the MVs is within the Miocene succession beneath the thick layer of Messinian Evaporites, in highly overpressured gas bearing stratigraphic traps at the Base Salt (Kirkham et al., 2022). A significant volume of methane gas would therefore be vented from these traps at the earliest stage of seal failure and hydraulic fracture propagation during conduit formation (Figs. 3A & 3B) (Kirkham et al., 2018), similar to gas mounds in the Gulf of Mexico that emanate from methane gas bearing sands (Meazell and Flemings, 2022). Methane is far more buoyant than the water in the trap, so it is reasonable to propose that the hydraulic fractures would have been largely driven upwards under gas buoyancy pressure (c.f. Nunn and Meulbroek (2002)) and the high mobility of the gas phase would lead to a concentration of methane in the initial flux up the conduits (Figs. 3A & 3B). As the height of the conduits grew, so did the connected gas column height within the conduit, providing additional buoyancy pressure at the fracture tips, which would peak at the seafloor (Fig. 3A). The absence of a clear crater at the base of a subset of MVs (Fig. 2B) indicates that their initial eruption was comparatively less vigorous than the MVs with craters (Fig. 2A), which by association could imply a lesser concentration of methane gas in their eruptive flux, as can occur across MVs (Mazzini and Etiope, 2017). Following the initial eruption, cyclicity in eruptive vigour is commonly observed during mud volcanism, with occasional increases in methane gas flux leading to the ignition of gas flares (Deville and Guerlais, 2009; Mazzini et al., 2021).

The MVs of the El Dabaa Province are unexceptional from a volcanic plumbing context, and share with the vast majority of MVs worldwide a close association with gas in the source regions. It seems likely that many other MVs are built on a foundation of a basal crater that has gone undetected because of data quality or sampling methodology, and the examples shown here may prompt re-examination of other suitable datasets for evidence of a highly vigorous initial phase of mud volcanism.

Conclusions

(1) Craters with diameters up to 2850m and relief >150 m are reliably interpreted at the basal surface of recently erupted MVs offshore Egypt.

(2) The genesis of the basal craters is best explained by a vigorous initial eruption during the onset of mud volcanism that excavated near surface sediments, with local slope failure modifying the final crater geometry.

(3) The energy for such vigorous eruption is driven by the concentration of methane in the initial flux. Gas buoyancy from a connected column upward through the hydraulic fracture network provides an additional overpressure drive.

Acknowledgements

We would like to thank Editor Gerry Dickens and 3 anonymous reviewers whose detailed comments significantly improved this paper. We thank Equinor for provision of the 3D seismic data and Schlumberger for providing academic licenses for their seismic interpretation software Petrel. Lastly, we acknowledge Mike Cassidy for giving helpful insight into analogous magmatic processes to those discussed here.

Figure captions

Figure 1. Location and stratigraphy of the western Nile Deep Sea Fan (NDFS). (A) Bathymetric map (from GeoMapApp, www.geomapapp.org) of the Eastern Mediterranean showing the location of the seismic study area (blue polygon) and the margins of the salt basin (pink line; modified from Lofi et al. (2011)). (B) Regional cross-section (Fig. 1A for location; modified from Kirkham et al. (2022)) from the western Nile Delta to the western NDSF, highlighting key marker horizons and stratigraphic units. Plio-Rec. – Pliocene-Recent; Mess. Evap. – Messinian Evaporites; MES – Messinian erosional surface. (C)

Seafloor map in the 3D seismic survey area (Fig. 1A for location), highlighting 86 mud volcanoes (MVs). (D) A seismic cross-section (Fig, 1C for location) showing MVs distributed throughout the Pliocene-Recent, truncation at the basal surface of some and depletion zones in the Oligo-Miocene underlying the MV. Older MVs (dashed light brown line) have been buried, compacted and undergone greater deformation compared to more recently erupted MVs (dashed white line).

Figure 2. Seismic character of craters at the base of mud volcanoes. (A) Seismic cross-section (Fig. 2C for location) through a mud volcano (MV) with a crater at its basal surface that truncates the underlying stratigraphy. (B) Seismic cross-section (Fig. 2D for location) through a MV that does not have a crater at its base. A conduit underlies the centre of the MV. (C) Map of the MV base in Fig. 2A. Points t-z highlight the margins of the MV and scarps at its basal surface and correlate with the cross-section in Fig. 2C. (D) Map of the MV base in Fig. 2B. Points 1-4 highlight the margins of the MV and its conduit and correlate with the cross-section in Fig. 2C. (E) A diameter vs relief plot for the basal craters.

Figure 3. A model for the genesis of craters at the base of mud volcanoes. (A) Upward propagation of hydraulic fractures through the Messinian Evaporites and Pliocene-Recent from the highly overpressured Oligo-Miocene. The initial flux up the conduit is dominated by water and methane. Buoyancy pressure from methane increases upward through the connected fracture column. (B) The conduit pierces the seafloor and there is a vigorous eruption of highly pressured gas and water that excavates a large crater. Local retrogressive slope failure could further modify the crater geometry. (C) Mud slurry buries the basal crater. Mud remobilisation from beneath the Base Salt synchronous to mud extrusion forms a depletion zone and causes the overburden to subside.

References

Barr, K., and Bolli, H. J. C. Q., 1953, The mud volcanoes of Trinidad: A Journal of Caribbean Culture, v. 3, no. 2, p. 80-85. https://doi.org/10.1080/00086495.1953.11829518

Davies, R. J., Brumm, M., Manga, M., Rubiandini, R., Swarbrick, R., Tingay, M. J. E., and Letters, P. S., 2008, The East Java mud volcano (2006 to present): an earthquake or drilling trigger?: Earth and Planetary Science Letters, v. 272, no. 3-4, p. 627-638. https://doi.org/10.1016/j.epsl.2008.05.029

Deville, E., and Guerlais, S.-H., 2009, Cyclic activity of mud volcanoes: evidences from Trinidad (SE Caribbean): Marine and Petroleum Geology, v. 26, no. 9, p. 1681-1691. https://doi.org/10.1016/j.marpetgeo.2009.03.002

Dolson, J., 2020, The Petroleum Geology of Egypt and History of Exploration. In: Hamimi Z., El-Barkooky A., Martínez Frías J., Fritz H., Abd El-Rahman Y. (eds) The Geology of Egypt. Regional Geology Reviews., The Geology of Egypt, Springer, p. 635-658.

Geshi, N., Németh, K., and Oikawa, T., 2011, Growth of phreatomagmatic explosion craters: a model inferred from Suoana crater in Miyakejima Volcano, Japan: Journal of Volcanology and Geothermal Research, v. 201, no. 1-4, p. 30-38. https://doi.org/10.1016/j.jvolgeores.2010.11.012

Higgins, G. E., and Saunders, J. B., 1974, Mud volcanoes—their nature and origin: Verh. Naturforsch. Ges. Basel, v. 84, p. 101-152.

Kellner, A., Brink, G., and El Khawaga, H., 2018, Depositional history of the western Nile Delta, Egypt: Late Rupelian to Pleistocene: AAPG Bulletin, v. 102, no. 9, p. 1841-1865. https://doi.org/10.1306/02161817234

Kirkham, C., Cartwright, J., Hermanrud, C., and Jebsen, C., 2017, The spatial, temporal and volumetric analysis of a large mud volcano province within the Eastern Mediterranean: Marine and Petroleum Geology, v. 81, p. 1-16. https://doi.org/10.1016/j.marpetgeo.2016.12.026

Kirkham, C., Cartwright, J., Hermanrud, C., and Jebsen, C., 2018, The genesis of mud volcano conduits through thick evaporite sequences: Basin Research, v. 30, no. 2, p. 217-236. https://doi.org/10.1111/bre.12250

Kirkham, C., Cartwright, J., James, D., and Kearney, L., 2022, Episodic venting of extreme subsalt overpressure through a thick evaporitic seal: Marine and Petroleum Geology, p. 105741. https://doi.org/10.1016/j.marpetgeo.2022.105741

Kopf, A., Robertson, A., Clennell, M., and Flecker, R., 1998, Mechanisms of mud extrusion on the Mediterranean Ridge Accretionary Complex: Geo-Marine Letters, v. 18, no. 2, p. 97-114. https://doi.org/10.1007/s003670050058

Krijgsman, W., Hilgen, F. J., Raffi, I., Sierro, F., and Wilson, D., 1999, Chronology, causes and progression of the Messinian salinity crisis: Nature, v. 400, no. 6745, p. 652-655. https://doi.org/10.1038/23231

Kugler, H. G., 1933, Contribution to the knowledge of sedimentary volcanism in Trinidad: Journal of the Institute of Petroleum Geology of Trinidad, v. 19, p. 743-772.

Lofi, J., Sage, F., Déverchère, J., Loncke, L., Maillard, A., Gaullier, V., Thinon, I., Gillet, H., Guennoc, P., and Gorini, C., 2011, Refining our knowledge of the Messinian salinity crisis records in the offshore domain through multi-site seismic analysis: Bulletin de la Société géologique de France, v. 182, no. 2, p. 163-180. https://doi.org/10.2113/gssgfbull.182.2.163

Loncke, L., Mascle, J., and Parties, F. S., 2004, Mud volcanoes, gas chimneys, pockmarks and mounds in the Nile deep-sea fan (Eastern Mediterranean): geophysical evidences: Marine and Petroleum Geology, v. 21, no. 6, p. 669-689. https://doi.org/10.1016/j.marpetgeo.2004.02.004

Løseth, H., Wensaas, L., Arntsen, B., Hanken, N.-M., Basire, C., and Graue, K., 2011, 1000 m long gas blow-out pipes: Marine and Petroleum Geology, v. 28, no. 5, p. 1047-1060. https://doi.org/10.1016/j.marpetgeo.2010.10.001

Mascle, J., Mary, F., Praeg, D., Brosolo, L., Camera, L., Ceramicola, S., and Dupré, S., 2014, Distribution and geological control of mud volcanoes and other fluid/free gas seepage features in the Mediterranean Sea and nearby Gulf of Cadiz: Geo-Marine Letters, v. 34, no. 2-3, p. 89-110. https://doi.org/10.1007/s00367-014-0356-4

Mazzini, A., Akhmanov, G., Manga, M., Sciarra, A., Huseynova, A., Huseynov, A., Guliyev, I. J. E., and Letters, P. S., 2021, Explosive mud volcano eruptions and rafting of mud breccia blocks: Earth and Planetary Science Letters, v. 555, p. 116699. https://doi.org/10.1016/j.epsl.2020.116699

Mazzini, A., and Etiope, G., 2017, Mud volcanism: An updated review: Earth-Science Reviews, v. 168, p. 81-112. https://doi.org/10.1016/j.earscirev.2017.03.001

Mazzini, A., Svensen, H., Akhmanov, G., Aloisi, G., Planke, S., Malthe-Sørenssen, A., and Istadi, B., 2007, Triggering and dynamic evolution of the LUSI mud volcano, Indonesia: Earth and Planetary Science Letters, v. 261, no. 3, p. 375-388. https://doi.org/10.1016/j.epsl.2007.07.001

Meazell, P. K., and Flemings, P. B., 2022, The evolution of seafloor venting from hydrate-sealed gas reservoirs: Earth and Planetary Science Letters, v. 579, p. 117336. https://doi.org/10.1016/j.epsl.2021.117336

Milkov, A. V., 2005, Global distribution of mud volcanoes and their significance in petroleum exploration as a source of methane in the atmosphere and hydrosphere and as a geohazard: Mud Volcanoes, geodynamics seismicity, p. 29-34. https://doi.org/10.1007/1-4020-3204-8_3

Nunn, J. A., and Meulbroek, P., 2002, Kilometer-scale upward migration of hydrocarbons in geopressured sediments by buoyancy-driven propagation of methane-filled fractures: AAPG bulletin, v. 86, no. 5, p. 907-918. https://doi.org/10.1306/61EEDBD4-173E-11D7-8645000102C1865D

Prinzhofer, A., and Deville, E., 2013, Origins of hydrocarbon gas seeping out from offshore mud volcanoes in the Nile delta: Tectonophysics, v. 591, p. 52-61. https://doi.org/10.1016/j.tecto.2011.06.028

Robertson, A., 1996, Mud volcanism on the Mediterranean Ridge: Initial results of ocean drilling program Leg 160: Geology, v. 24, no. 3, p. 239-242. https://doi.org/10.1130/0091-7613(1996)024

Ryan, W. B., 2009, Decoding the Mediterranean salinity crisis: Sedimentology, v. 56, no. 1, p. 95-136. https://doi.org/10.1111/j.1365-3091.2008.01031.x

Stewart, S. A., and Davies, R. J., 2006, Structure and emplacement of mud volcano systems in the South Caspian Basin: AAPG bulletin, v. 90, no. 5, p. 771-786. https://doi.org/10.1306/11220505045

Tingay, M., Rudolph, M., Manga, M., Davies, R., and Wang, C.-Y., 2015, Initiation of the Lusi mudflow disaster: Nature geoscience, v. 8, no. 7, p. 493-494. https://doi.org/10.1038/ngeo2472

Figure 1

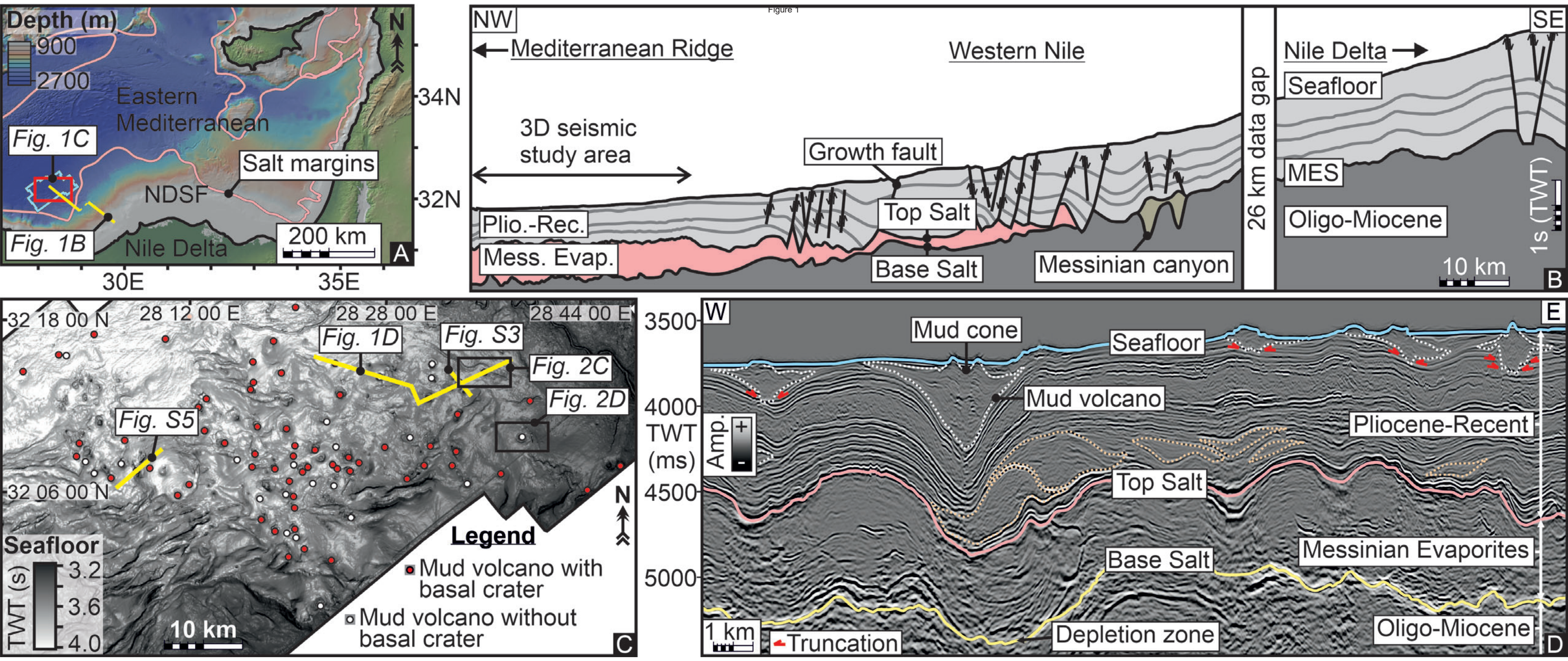

Depth (m)
900
2700
N
34N
32N
30E
35E
Eastern Mediterranean
Fig. 1C
Salt margins
NDSF
Fig. 1B
Nile Delta
200 km
A
NW
Mediterranean Ridge
Western Nile
3D seismic study area
Growth fault
Top Salt
Plio.-Rec.
Mess. Evap.
Base Salt
Messinian canyon
26 km data gap
SE
Nile Delta
Seafloor
MES
Oligo-Miocene
1s (TWT)
10 km
B
32 18 00 N
28 12 00 E
28 28 00 E
28 44 00 E
Fig. 1D
Fig. S3
Fig. 2C
Fig. 2D
Fig. S5
32 06 00 N
Seafloor
TWT (s)
3.2
3.6
4.0
10 km
N
Legend
Mud volcano with basal crater
Mud volcano without basal crater
C
W
E
3500
4000
4500
5000
TWT (ms)
Amp.
+
-
Mud cone
Seafloor
Mud volcano
Pliocene-Recent
Top Salt
Messinian Evaporites
Base Salt
Depletion zone
Oligo-Miocene
1 km
Truncation
D

Figure 2

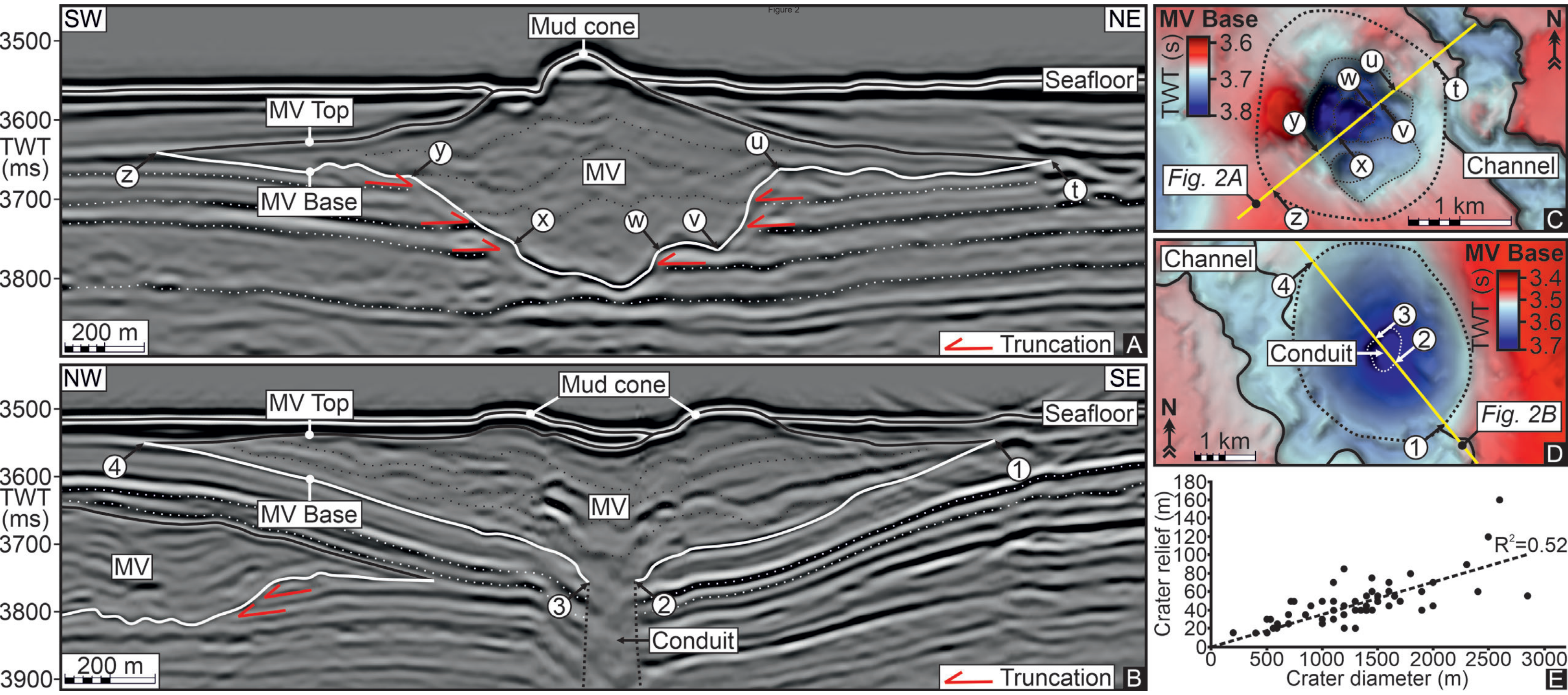
SW
NE
Mud cone
Seafloor
MV Top
MV Base
MV
z
y
x
w
v
u
t
3500
3600
TWT
(ms)
3700
3800
200 m
Truncation
A
NW
SE
Mud cone
MV Top
MV Base
MV
Seafloor
4
3
2
1
Conduit
3500
3600
TWT
(ms)
3700
3800
3900
200 m
Truncation
B
MV Base
TWT (s)
3.6
3.7
3.8
Fig. 2A
Channel
1 km
N
C
Channel
MV Base
TWT (s)
3.4
3.5
3.6
3.7
Conduit
Fig. 2B
1 km
N
D
Crater relief (m)
Crater diameter (m)
R²=0.52
0
20
40
60
80
100
120
140
160
180
0
500
1000
1500
2000
2500
3000
E

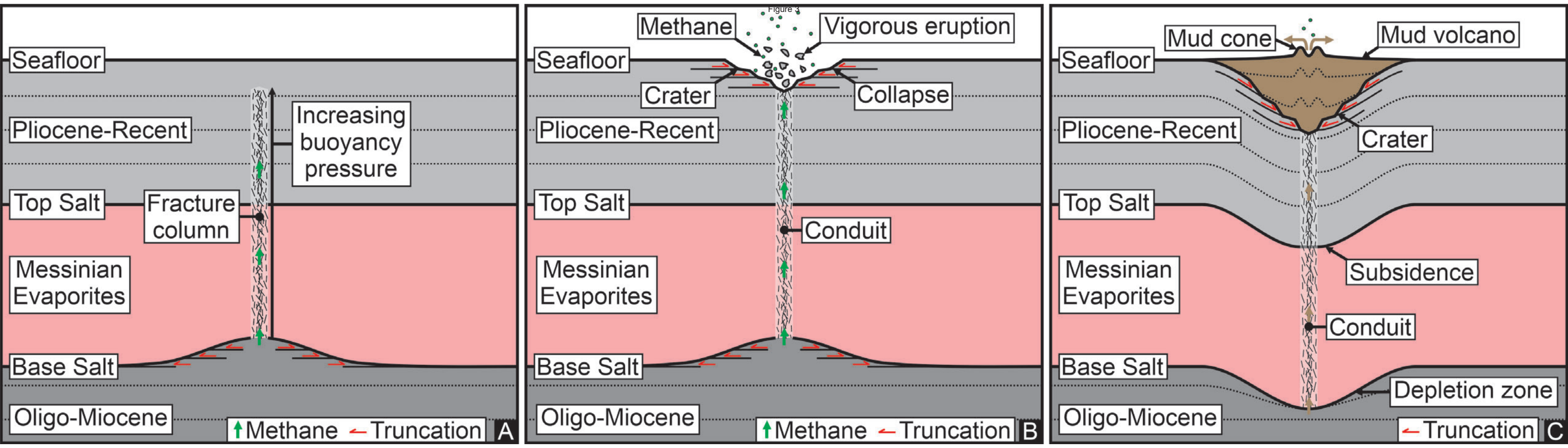
Figure 3
Seafloor
Pliocene-Recent
Increasing
buoyancy
pressure
Top Salt
Fracture
column
Messinian
Evaporites
Base Salt
Oligo-Miocene
Methane
Truncation
A
Methane
Vigorous eruption
Seafloor
Crater
Collapse
Pliocene-Recent
Top Salt
Conduit
Messinian
Evaporites
Base Salt
Oligo-Miocene
Methane
Truncation
B
Mud cone
Mud volcano
Seafloor
Pliocene-Recent
Crater
Top Salt
Subsidence
Messinian
Evaporites
Conduit
Base Salt
Depletion zone
Oligo-Miocene
Truncation
C